

SUPPLEMENTARY TABLES AND FIGURES

Supplementary Table 1. The list of podocyte genes selected for capture.

Supplementary Table 2. Fisher's Exact Test for single variants in patients vs. controls.

Supplementary Table 3. Burden test of rare variants in FSGS cases vs. controls.

The rare variants are 5662 missense and loss of function variants in our dataset that are present at a frequency of $< 1/10,000$ in the European population in the ExAC database.

Supplementary Table 4. Complete list of rare variant analyses by variable threshold test and C-alpha test.

Supplementary Table 5. The list of 20 known FSGS risk genes used.

Supplementary Table 6. A complete list of missense or loss of function variants in known FSGS risk genes. These variants have $MAF < 0.1$ in European American cases and controls, and $OR > 1$.

Supplementary Table 7. Variant distribution from our sequencing analyses.

Supplementary Figure 1. (A) 2500 podocyte specific genes were selected and referred to as the "podocyte exome". (B) Average sequencing coverage for all cases in FSGS cases. Each bar represents the coverage of a patient DNA sample we sequenced. (C) Gene network analysis showed 3 clusters of FSGS risk genes: Actin cytoskeleton regulators, glomerular basement membrane components, and slit diaphragm components.

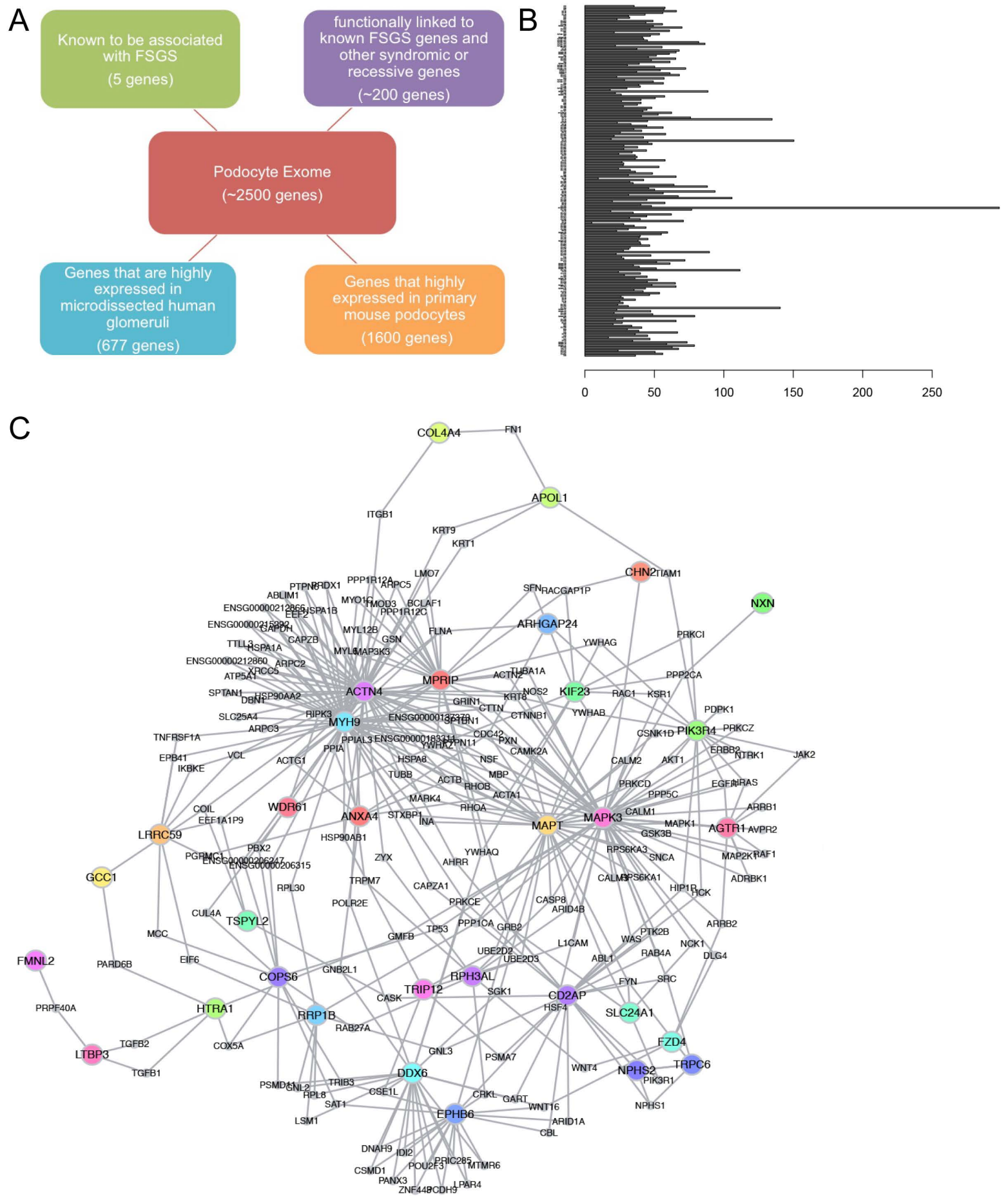
Supplementary Figure 2. (A) The efficiency of three miR30-shRNAs targeted against Cd2ap. A mouse CD2AP-EGFP vector was co-expressed with different miR30-shRNA constructs in HEK293 cells. The expression level of CD2AP-EGFP was detected by immunoblotting. Actin immunoblotting was used as loading control. FF3, a miR30-shRNA that targeted fire fly luciferase was used as control. Cd2ap and actin blots were run with duplicate samples run on parallel gels. (B) PCR validation of homologous recombination. The design of genomic PCR and the example of results that validated homologous recombination in ES clones. Forward primer (P1: 5'-CAAGCCCGGTGCCTGATCTAGATCATAATC-3') was designed at the end of puromycin resistant cassette. Two reverse primers were designed outside the Right Arm. (P2: 5'-CTGTAAAGGTCTCTGAACTACCAATTGCAC-3', and P3: 5'-GAGACTAAGGCAGGAGGATTCCAGGTTTG -3'). The arrows denote the specific

PCR products for the PCR reactions by using P1+P2 and P1+P3. The veracity of the PCR products were confirmed by restriction digestion. (C) A schematic of the podocyte-specific, DOX-inducible RNAi system. (D) *Cd2ap*-RNAi mice showed DOX-dependent proteinuria. DOX treatment was stopped after 8 weeks. Urine samples were collected at 4, 8, 12 and 16-week time points. Albumin/creatinine ratios were measured and plotted. (E) By electron microscopy, doxycycline dependent foot process effacement was present in *Cd2ap*-RNAi mice, while podocyte cytoarchitecture was preserved in control mice.

Supplementary Figure 3. (A) The method developed to test the RNAi efficiency of a given miR30-shRNA. The Exon targeted by the shRNA (ExonX) was amplified by genomic PCR and inserted into the 3' end of the EGFP sequence in the pEGFP-C1 vector. The pEGFP-C1-ExonX was then used as an artificial target for the shRNA. The pEGFP-C1-ExonX and miR30-shRNA constructs were co-expressed in 293 cells, and the expression level of EGFP was detected by immunoblotting. (B) Immunoblotting results for each miR30-shRNA oligo designed for the candidate genes. The FF3 miR30-shRNA was used as control for each miR30-shRNA oligo. Actin immunoblotting was used as a loading control. The expression of EGFP was used as an indicator for RNAi efficiency. The miR30-shRNA oligo that had the best RNAi efficiency was inserted into the pHPRT targeting vector to generate RNAi ES cells and mice. Some of the blots are also shown in Figure 4A.

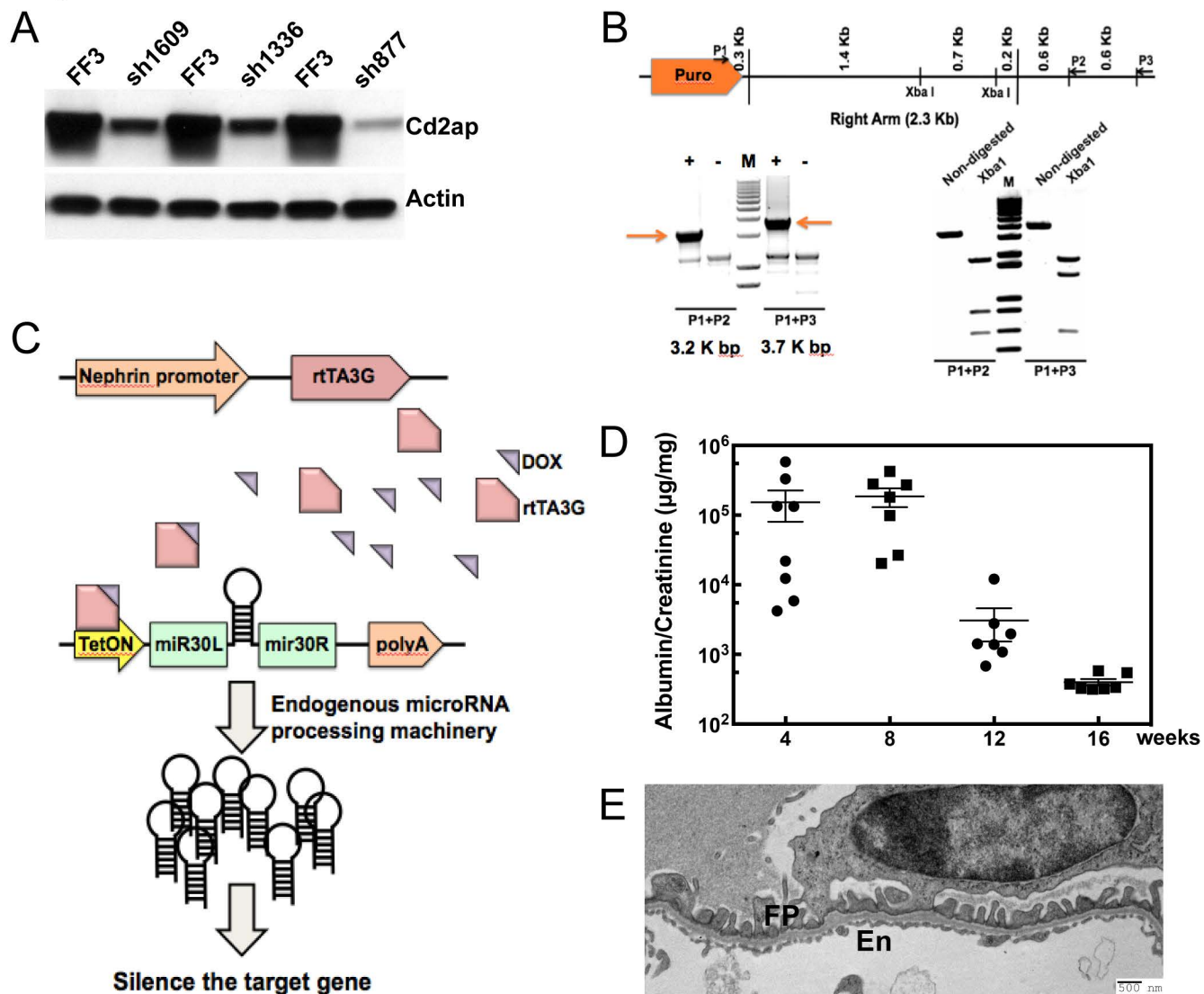
Supplementary Figure 4. (A) *Dlg5*- and *Kat2b*-RNAi mice showed no proteinuria after 12 weeks of DOX treatment, while *Kank1*-RNAi mice showed significant proteinuria at the 12 week time point. (B) *Dlg5* heterozygosity did not accelerate the development of proteinuria in *CD2AP*^{-/+}, *Synpo*^{-/+} mice. Urines were collected at the indicated time points and albumin/creatinine measured. (C) Electron microscopy images of glomeruli from *Arhgef17*⁻, *Kank1*⁻, *Kank2*⁻ and *Wnk4*-RNAi mice showed the foot process effacement. The foot process of *Dlg5*- and *Kat2b*-RNAi mice are largely normal.

Figure S1



Supplementary Figure 1. (A) 2500 genes were clustered and defined as “podocyte exome”. (B) Average sequencing coverage for all cases in FSGS cases. Each bar represents the coverage of a patient DNA sample we sequenced. (C) Gene network analysis showed 3 clusters of FSGS risk genes: Actin cytoskeleton regulators, glomerular basement membrane components, and slit diaphragm components.

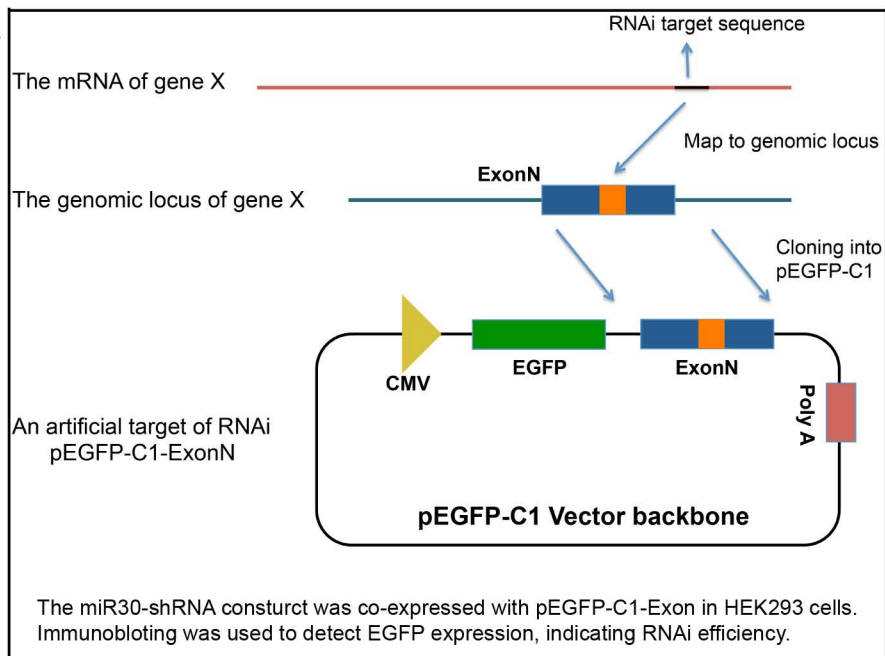
Figure S2



Supplementary Figure 2. (A) The efficiency of 3 miR30-shRNAs that targets Cd2ap. A mouse CD2AP-EGFP vector was co-expressed with different miR30-shRNA constructs in HEK293 cells. The expression level of CD2AP-EGFP was detected by immunoblotting. Actin immunoblotting was used as loading control. FF3, A miR30-shRNA that targets fire fly luciferase was used as control. The design of genomic PCR and the example of results that validate homologous recombination in ES clones. Forward primer (P1: 5'-CAAGCCCGGTGCCTGATCTAG ATCATAATC-3') was designed at the end of puromycin resistant cassette. Two reverse primers were designed outside the Right Arm. (P2: 5'-CTGTAAAGGTCTCTGAACTACCAATTGCAC-3', and P3: 5'-GAGACTAAGGCAGGAGGATTCCAGGTTTG -3'). (B) PCR validation of homologous recombination. The arrows point to the specific PCR products for the PCR reactions by using P1+P2 and P1+P3, and the PCR products were confirmed by restriction digestion with desired sizes of digested DNA fragments. (C) The system of podocyte-specific, DOX-inducible RNAi. (D) Cd2ap-RNAi mice showed DOX-dependent proteinuria. The DOX treatment was stopped after 8 weeks. The urine samples were collected at 4, 8, 12 and 16-week time points. Albumin/creatinine ratio was measured and plotted. (E) By electron microscopy, doxycycline dependent foot process effacement was present in Cd2ap-RNAi mice, while podocyte cytoarchitecture is preserved in control mice.

Figure S3

A



B

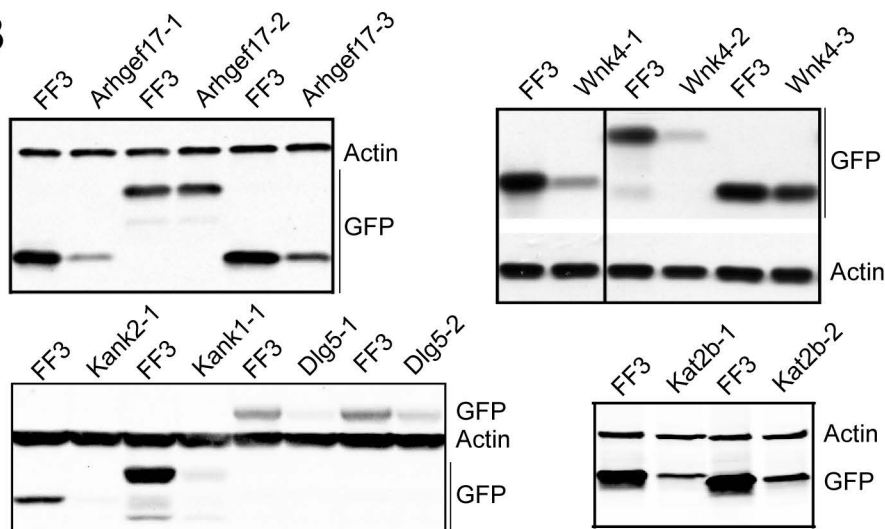


Figure S4

